ELSEVIER

Journal of Chromatography A, 829 (1998) 309–315

JOURNAL OF CHROMATOGRAPHY A

Fluorescence detection of proteins and amino acids in capillary electrophoresis using a post-column sheath flow reactor

Paula G. Coble, Aaron T. Timperman[1,*]

University of South Florida, Department of Marine Science, St. Petersburg, FL 33701, USA

Received 25 March 1998; received in revised form 29 September 1998; accepted 29 September 1998

Abstract

A simple laser-induced fluorescence detection method for proteins and amino acids in capillary electrophoresis is reported. A sheath flow cell is utilized as a post-column reactor for fluorescence derivatization of proteins and amino acids by addition of *o*-phthaldialdehyde–2-mercaptoethanol to the sheath fluid. With the use of a 50 μm I.D. capillary, the limits of detection for carbonic anhydrase are 0.73 n*M* or 1.8 amol which represents a five- and two-fold improvement, respectively, over the best results previously reported for post-column detection. In addition, separation efficiencies up to $8.07 \cdot 10^5$ are achieved, and the detector response is linear over three-orders of magnitude. These results demonstrate that mixing is adequate and the reaction kinetics are rapid enough to provide sensitive detection with this approach. Also, because this post-column derivatization scheme requires no instrumental changes to a typical sheath flow cell detector, the system can be used for detection of pre-column labeled analytes and for native fluorescence detection.

Keywords: Detection, electrophoresis; Fluorescence detection; Proteins; Amino acids

1. Introduction

Laser-induced fluorescence (LIF) detectors have produced very impressive mass limits of detection (LODs) for highly fluorescent model fluorophores. Dovichi and co-workers used a sheath flow cell LIF detection system to produce the lowest reported detection limits for capillary electrophoresis (CE) at six molecules of sulforhodamine 101 [1], and single molecules of B-phycoerythrin [2]. However, detection limits are much worse for real biological samples which exhibit very weak native fluorescence when compared with model fluorophores, such as fluorescein and sulforohodamine. Native fluorescence detection of proteins relies primarily on the presence of fluorescent tryptophan or tyrosine residues, and has produced detection limits down to $1 \cdot 10^{-10}$ *M* for conalbumin [3]. For fluorescence tagging of complex environmental and biological samples, post-column detection is advantageous since it does not complicate the separation. Pre-column derivatization can result in separation of heterogeneously labeled analytes, yielding multiple peaks for a single analyte species [4–7]. Furthermore, pre-column derivatization gives rise to large fluorescent backgrounds from excess highly fluores-

*Corresponding author. Corresponding address: University of Washington, 1705 NE Pacific, K-363, Seattle, WA 98195-7730, USA. Tel.: +1-206-221-4196, Fax: +1-206-685-7301.

[1]Present address: University of Washington, Seattle, WA 98195-7730, USA.

0021-9673/98/$ – see front matter
PII: S0021-9673(98)00799-7

cent reagents and their by-products, which obscure large portions of the baseline and make derivatization of dilute samples impossible. Thus, we have chosen to avoid pre-column derivatization due to the increased complexity and obscuration of large regions of the electropherograms.

Recently an ingenious approach to pre-column derivatization has been used to achieve the lowest reported detection limits for native proteins through co-elution of heterogeneously labeled proteins. In this work, Dovichi et al. [8] used 5-furoylquinoline-3-carboxaldehyde for pre-column derivatization, and co-elution of heterogeneous multiply labeled proteins was achieved through addition of sodium dodecyl sulfate below the critical micellar concentration. With this scheme, detection limits as low as $5 \cdot 10^{-11}$ *M* were achieved for conalbumin which is a 10-fold improvement of the detection limits reported here. Although this method is capable of producing low detection limits, it is limited by regions of the electropherogram which are obscured by fluorescent by-products, and it is not capable of resolving different glycoforms of glycoproteins or other micro-heterogeneity.

For a post-column detection scheme to be successful it must introduce the derivatizing agents and detect the labeled analytes with minimal band broadening or degradation of detection limits through dilution of the sample. Most previous approaches to post-column derivatization introduce the derivatizing reagents through a gap junction. Gap junction reactors have been fabricated using tee connectors [9,10], in-line capillaries [11–13], and coaxial capillaries [5,14,15], which introduce the fluorescence derivatization solution using hydrodynamic pressure [5,9–11,14] or electroosmotic flow [13,15] or diffusion [12]. Yeung and Zhang [15] utilized a coaxial gap reactor which added the reactants by electroosmotic pumping, yielding detection limits of $3.8 \cdot 10^{-9}$ *M* or 3.8 amol for carbonic anhydrase with a separation efficiency of 190 000.

The current work utilizes a novel sheath flow cell reactor for direct analysis of complex and dilute protein samples. No changes in the instrumentation or design of a typical LIF sheath flow cell are required; the only change required is the addition of the fluorescent derivatizing agents to the sheath fluid. Sheath flow reactors have been used for chemiluminescence detection [16–18] and LIF detection of amino acids [19] in CE, but not for detection of proteins. *o*-Phthaldialdehyde (OPA)–2-mercaptoethanol chemistry is well-suited and widely used for post-column derivatization, due to its fluorogenic nature [20] and fast reaction kinetics [21,22]. With this sheath flow cell reactor, fast reaction kinetics are extremely important as reaction times are about 1–2 s.

2. Experimental

2.1. Detection system

The detection system utilizes high-efficiency light collection, a sheath flow cell, and a photon counting photomultiplier tube (PMT) to provide low detection limits. A schematic of the sheath flow cell and optical set-up of the detector is shown in Fig. 1. Two He–Cd lasers were used for excitation; the work was initiated with a 354 nm He–Cd (Model 7205, LiConix, Santa Clara, CA, USA) which did not function reliably, and the data presented here were acquired using a 325 nm He–Cd (Model 3211N, LiConix) which was more reliable. The laser excitation is passed through a prism and an iris to remove

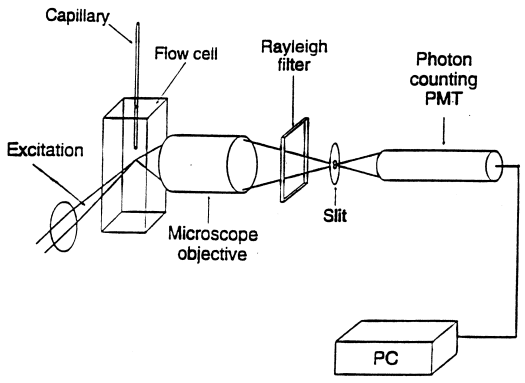

Fig. 1. A schematic of the sheath flow post-column reactor is shown. The sheath fluid, which contains the OPA–2-mercaptoethanol enters from the top of the flow cell and surrounds the capillary eluent as it exits the capillary. A 325 nm He–Cd laser is used for fluorescence excitation. The fluorescence emission is collected with a microscope objective and focused onto the slit before. A photon counting PMT module is used for detection and the data is recorded by the computer.

laser tube background before it is focused onto the capillary. A 50-mm focal length plano convex lens (Spindler & Hoyer, Milford, MA, USA) is used for focusing the excitation into a spot at the detection window.

The sheath flow cell is made of a quartz flow cell with a square cross-section of 0.5 mm, 1 mm thick walls, and length of 25 mm (Hellma Cells, Forest Hills, NY, USA). The end of the capillary is polished to a point using a high speed rotary grinder, and is centered in the flow cell. The sheath fluid is filtered with an in-line filter degasser (Aqueous IFD, Whatman, Maidstone, UK) before it is introduced into the flow cell body, and the plumbing for the sheath fluid is achieved with standard low-pressure fittings. The sheath fluid is hydrodynamically pumped using a vertical displacement of 4 cm, yielding a linear flow-rate of 3 mm/s in the detection window. To prevent contamination with background fluorescence and bacterial growth, the sheath flow system is flushed nightly with HPLC-grade methanol.

The fluorescence is collected with a long working distance, 60× magnification, 0.65 NA microscope objective (MO-0060LWD, Universe Kogaku, Oyster Bay, NY, USA). The collected emission is filtered with a 420 nm high-pass absorptive glass filter to remove Rayleigh and Raman scattering (SGG-420, CVI Laser Corp., Albuquerque, NM, USA). The light is then focused on a variable iris with a minimum aperture of 1 mm. After passing through the iris the emission passes onto the face of the PMT.

The HC135-01 photon counting PMT module (Hamamatsu, Middlesex, NJ, USA) includes a microcontroller and high voltage power supply. The PMT module is an excellent choice for this system as it combines good figures of merit, and is easy to use. The counting efficiency ranges from 20% to 10% and the equivalent noise index is less than $5 \cdot 10^{-16}$ W over the 420–520 nm spectral region. A crystal-controlled counter/timer and microcontroller integrates the signal into precise 10-ms intervals which can be summed. An algorithm corrects for PMT dead time to remove non-linearity at high count rates, yielding a linear dynamic range of $2 \cdot 10^{6}$.

A Gateway 2000 P5-75 computer and an ATMIO-16E-10 multifunction I/O board are used for data acquisition and system control. Data acquisition is controlled with a C program written in the laboratory using Lab Windows CVI (National Instruments, Austin, TX, USA). The integrated signal is transferred from the PMT microcontroller to the computer via the serial port. The C program controls the number of 10-ms time intervals to be summed into a single read, and a 30 ms integration period is used for the presented data.

2.2. Electrophoresis system

The separation potential is applied with a 30 kV high-voltage power supply (Glassman, Whitehouse Station, NJ, USA). A separation potential of 20 kV is used for all electropherograms, and is remotely controlled by the data acquisition program. Due to the sheath flow cell design, the detection end is held at ground while the injection end is connected to the positive potential. Pt electrodes are used to complete the electrical circuit at both the capillary inlet and outlet. At the capillary outlet the electrode is housed in a chamber that collects bubbles produced by electrolysis at the capillary outlet. These bubbles are purged about once every 10 runs with sheath fluid by opening a valve in the top of the electrode chamber. To minimize band broadening the sheath inlet, and capillary inlet and outlet are all at the same vertical height. The injection end is enclosed in a Plexiglas box with high voltage safety interlocks, and the capillary is insulated with PTFE and Tygon tubing between the injection box and the sheath flow cell mount. The amino acids are run in both bare fused-silica capillaries (Polymicro Technologies, Phoenix, AZ, USA) and deactivated capillaries (Scientific Resources, Eatontown, NJ, USA); while acrylamide polymer coated capillaries (Scientific Resources), ethylene glycol coated capillaries (Scientific Resources), and deactivated capillaries are tested for use in the protein separations. All capillaries had dimensions of 54 cm×50 μm I.D.×350 μm O.D.

2.3. Injections

All injections are 10 cm, 10 s hydrodynamic injections with a calculated injection volume of 2.4 nl. The sheath flow is turned off with a valve during injection so it does not apply back pressure to the capillary outlet during the injection, and is turned on

15 s after beginning the separation. Immediately after an injection, the capillary inlet is quickly dipped in a vial of clean running buffer (at the same height as the injection vial) to minimize the effects of extraneous injection. All sample solutions are prepared in running buffer, so no focusing or stacking effects are present.

2.4. Reagents

All solutions are prepared using ultrapure Milli-Q water (Millipore, Bedford, MA, USA), and all buffer salts and glassware are baked at 500°C for 12 h to remove organic contaminants. The pH 9.5, 50 m*M* borate buffer for the sheath fluid and running is made by dissolving 4.78 g of ACS-reagent-grade sodium tetraborate decahydrate (Sigma), adding about 45 ml of 0.200 *M* NaOH, and diluting to a final volume of 1.00 l with water. pH measurements are made from a small portion of the buffer which is discarded after the measurement to avoid contamination of the buffer from the pH electrode. Prior to its use both the running and sheath fluid buffers are degassed using a rotary evaporator at a vacuum of 25 mmHg for 1 h (1 mmHg=133.322 Pa).

The OPA derivatization solution is prepared in a similar manner to previous methods used for post-column derivatization [12,23]. The solution consists of: 2 m*M* high purity OPA (Molecular Probes, Eugene, OR, USA), 8 m*M* 2-mercaptoethanol (biochemika grade, Fluka, Buchs, Switzerland), 3% high purity methanol (B & J Brand, Fluka), and degassed 50 m*M* borate buffer. The reagents are added in the order in which they are listed, and made fresh daily.

All of the protein and amino acid standards were purchased from Sigma and prepared in 50 m*M* borate buffer. The amino acid standards were: Sigma Ultra L-glycine (G-7403), L-phenylalanine (P-8324), Sigma Ultra L-serine (S-8407), L-tryptophan (T-0254) and L-tyrosine hydrochloride (T-2006). The protein standards were: carbonic anhydrase (C-2273), human apo-transferrin (T-0519), α-lactalbumin (L-6385), β-lactoglobulin B (L-8005), trypsin inhibitor from soybean (T-9767), β-lactoglobulin A (L-7880), pepsin from porcine stomach mucosa (P-1143), trypsinogen from bovine pancreas (T-9011).

2.5. Data treatment

The data shown in all three electropherograms is smoothed using Grams 386 for Chromatography (Galatic Industries, Salem, NH, USA) in order to obtain the maximum signal-to-noise ratio (S/N) without a degradation in separation efficiency. The best results are obtained with a second order Savitsky–Golay smoothing routine. All detection limits are calculated using the 3σ definition.

3. Results and discussion

3.1. Limits of detection and linearity

The LODs are determined for several protein standards as shown in Table 1. Carbonic anhydrase yields the lowest detection limits at $7.3 \cdot 10^{-10}$ *M* which is a five-fold improvement over the best previously reported results for post-column derivatization. An electropherogram of carbonic anhydrase with a $S/N=23$ is shown in Fig. 2. The LODs for the proteins cover a range of about one-order of magnitude, as would be expected for a derivatizing agent such as OPA in this detection system. These results demonstrate that this detection scheme provides an

Table 1
LODs and separation efficiencies of protein standards

Elution order	Protein	Concentration LOD (n*M*)	Mass LOD (amol)	*N*
1	Carbonic anhydrase	0.73	1.8	$3.4 \cdot 10^5$
2	Human apo-transferrin	1.4	3.3	$1.6 \cdot 10^5$
3	α-Lactalbumin	1.4	3.4	$8.1 \cdot 10^5$
4	β-Lactoglobulin B	9.7	23	$4.2 \cdot 10^4$
5	Trypsin inhibitor, soybean	5.7	14	$3.2 \cdot 10^5$
6	β-Lactoglobulin A	7.2	17	$7.6 \cdot 10^4$

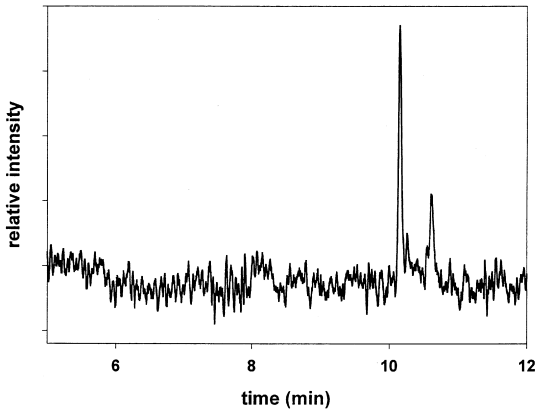

Fig. 2. An electropherogram of $5.3 \cdot 10^{-9}$ *M* carbonic that shows two different peaks which are inherent in the carbonic anhydrase standard. The LOD as calculated for the primary peak is $7.3 \cdot 10^{-10}$ *M* or 1.8 amol. The running buffer was 50 m*M* borate, pH 9.5, and the polyacrylamide coated capillary was 54 cm in length while a separation potential of 20 kV was used.

ample reaction time and mixing of the analytes and derivatizing reagents. The high fluorescent background produced by the OPA in the sheath fluid is the major contributor to baseline noise, as the baseline intensity increases by about two-orders of magnitude upon addition of OPA to the sheath fluid. The LODs for pepsin and trypsinogen are not reported since these standard proteins had numerous peaks; however, the total peak areas are comparable to those of the protein standards reported in Table 1. As with all OPA protein detection methods, free ϵ-amine groups of lysine residues are required for conjugation with OPA [24].

The performance of the detection system is effected by the detector integration period, the distance between the capillary outlet and the detection window, and the sheath flow velocity. Both 100 ms and 30 ms integration times are used for data collection, with 30 ms showing a 2.5-fold improvement over 100 ms after data smoothing. Therefore, a 30 ms detector integration period is used for all of the data reported here. The capillary outlet to detection window distance is varied from 1.5 mm to 3 mm to 5 mm, and a distance of 3 mm is found to provide both the lowest LODs and highest separation efficiencies. The optimum sheath flow-rate in the detection window is 3 mm/s as it yields the lowest LODs and most uniform peak shapes. With a linear flow-rate of less than 3 mm/s the LODs increase and the baseline is unstable, while a linear flow-rate greater than 3 mm/s also increases the LODs and causes peak tailing.

Detection limits for amino acids are moderately higher than for proteins as shown in Table 2. Glycine yields the lowest LOD for amino acids, at $2.3 \cdot 10^{-8}$ *M* which is expected since it has the fastest reaction kinetics with OPA–2-mercaptoethanol [21]. In comparison, the detection limits for proteins are lower which can be attributed to labeling at multiple sites.

A log–log plot was constructed for a calibration curve and the detector gives a linear response over three-orders of magnitude. Concentrations of $5 \cdot 10^{-9}$ *M* to $5 \cdot 10^{-6}$ *M* carbonic anhydrase are used, and triplicate injections yield a correlation coefficient of 0.997. The response of $1 \cdot 10^{-6}$ *M* carbonic anhydrase exhibited a slight negative deviation from linearity. These results are favorable, as many post-column reactors display linearity over about two-orders of magnitude [12,15].

3.2. Separations

A separation of protein standards is shown in Fig. 3. An acrylamide polymer coated capillary is used in order to minimize interactions with the capillary walls. Although this capillary is coated with acrylamide, the electroosmotic flow is strong enough for

Table 2
LODs and separation efficiencies of amino acid standards

Elution order	Amino acid	Concentration LOD (n*M*)	Mass LOD (amol)	*N*
1	Tryptophan	22	52	$1.6 \cdot 10^5$
2	Glycine	12	28	$3.4 \cdot 10^5$
3	Phenylalanine	69	170	$4.0 \cdot 10^5$
4	Tyrosine	34	81	$4.4 \cdot 10^5$
5	Serine	32	77	$3.9 \cdot 10^5$

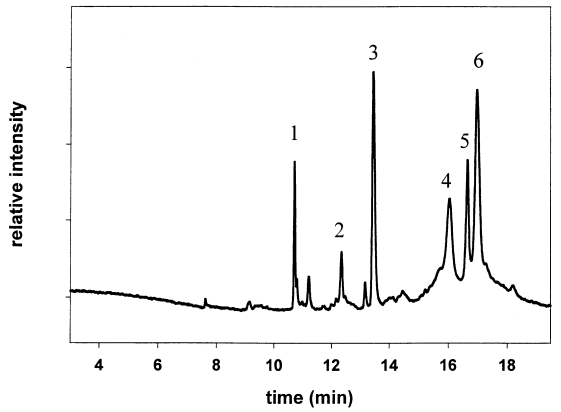

Fig. 3. A CE separation of: carbonic anhydrase [(1) $1.3\cdot10^{-7}$ *M*], apo-transferrin [(2) $1.0\cdot10^{-7}$ *M*], α-lactalbumin [(3) $5.0\cdot10^{-7}$ *M*], β-lactoglobulin B [(4) $1.0\cdot10^{-6}$ *M*], trypsin inhibitor [(5) $1.0\cdot10^{-6}$ *M*], β-lactoglobulin A [(6) $1.9\cdot10^{-6}$ *M*]. Separation conditions as in Fig. 2.

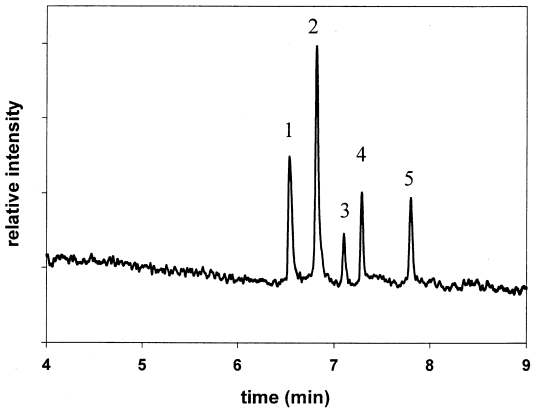

Fig. 4. A CE separation of tryptophan [(1) $1.0\cdot10^{-6}$ *M*], glycine [(2) $1.0\cdot10^{-6}$ *M*], phenylalanine [(3) $1.2\cdot10^{-6}$ *M*], tyrosine [(4) $1.1\cdot10^{-6}$ *M*], serine [(5) $1.0\cdot10^{-6}$ *M*]. Separation conditions as in Fig. 2, except a bare deactivated-silica capillary was used.

elution of these proteins which migrate toward the anode (inlet) under these conditions. Bare fused-silica, deactivated fused-silica and ethylene glycol coated capillaries [25] are found to give excessive amounts of band broadening with these protein standards. With the use of these capillaries and without the use of focusing or stacking techniques, a separation efficiency of over 800 000 is obtained for α-lactalbumin, as shown in Table 1. This result demonstrates that the detection system can provide high separation efficiencies and introduces minimal band broadening into the system. The lower separations efficiencies achieved for β-lactoglobulin A and for β-lactoglobulin B are most likely caused by greater sample–wall interactions or the presence of multiple protein states. The baseline hump which appears in Fig. 3 beneath the β-lactoglobulin B, β-lactoglobulin A and trypsin inhibitor peaks is found to be inherent in these samples and is caused by factors similar to those previously mentioned.

A separation of tryptophan, glycine, phenylalanine, tyrosine and serine (Fig. 4) shows baseline resolution between all of the amino acids. Separation efficiencies between 440 000 and 160 000 are achieved in a deactivated fused-silica capillary as shown in Table 2. The peaks are rather symmetric with very little tailing.

4. Conclusions

Through introduction of the sheath fluid under laminar flow conditions and minimal levels of background scattering, sheath flow cell reactors afford sensitive detection in spite of very short reaction times. The sheath flow post-column reactor reported here has achieved detection limits as low as $7.3\cdot10^{-10}$ *M* and separation efficiencies as high as 800 000 for native proteins. This post-column detector also has the additional advantages of a stable baseline which is free of fluorescent derivatization by-products and can resolve protein microheterogeneity.

Acknowledgements

We would like to thank the Office of Naval Research for funding (Grants N00014-94-1-0963 and N00014-94-1-5010).

References

[1] D.Y. Chen, K. Adelhelm, X.L. Cheng, N.J. Dovichi, Analyst 119 (1994) 349.
[2] D.Y. Chen, N.J. Dovichi, Anal. Chem. 68 (1996) 690.

[3] T.T. Lee, E.S. Yeung, J. Chromatogr. 595 (1992) 319.
[4] K.C. Chan, G.M. Janini, G.M. Muschik, H.J. Issaq, J. Liq. Chromatogr. 16 (1993) 1877.
[5] B. Nickerson, J.W. Jorgenson, J. Chromatogr. 480 (1989) 157.
[6] D.F. Swaile, M.J. Sepaniak, J. Liq. Chromatogr. 14 (1991) 869.
[7] J.Y. Zhao, K.C. Waldron, J. Miller, J.Z. Zhang, H. Harke, N.J. Dovichi, J. Chromatogr. 608 (1992) 239.
[8] D.M. Pinto, E.A. Arriaga, D. Craig, J. Angelova, N. Sharma, H. Ahmadzadeh, N.J. Dovichi, Anal. Chem. 69 (1997) 3015.
[9] T. Tsuda, Y. Kobayashi, A. Hori, T. Matsumoto, O. Suzuki, J. Chromatogr. 456 (1988) 375.
[10] S.L. Pentoney Jr., X. Huang, D.S. Burgi, R.N. Zare, Anal. Chem. 60 (1988) 2625.
[11] R. Zhu, W.T. Kok, J. Chromatogr. A 716 (1995) 123.
[12] S.D. Gilman, J.J. Pietron, A.G. Ewing, J. Microcol. Sep. 6 (1994) 373.
[13] M. Albin, R. Weinberger, E. Sapp, S. Moring, Anal. Chem. 63 (1991) 417.
[14] D.J. Rose, J.W. Jorgenson, J. Chromatogr. 447 (1988) 117.
[15] L. Zhang, E.S. Yeung, J. Chromatogr. A 734 (1996) 331.
[16] M.A. Ruberto, M.L. Grayeski, Anal. Chem. 64 (1992) 2758.
[17] R. Dadoo, L.A. Colon, R.N. Zare, J. High Resolut. Chromatogr. 15 (1992) 133.
[18] J.-Y. Zhao, J. Labbe, N.J. Dovichi, J. Microcol. Sep. 5 (1993) 331.
[19] K.E. Oldenburg, X.I. Xi, Analyst 122 (1997) 1581.
[20] M. Roth, Anal. Chem. 43 (1971) 880.
[21] V.-J.K. Svedas, I.J. Galaev, I.L. Borisov, I.V. Berezin, Anal. Biochem. 101 (1980) 188.
[22] R.F. Chen, C. Scott, E. Trepman, Biochim. Biophys. Acta 576 (1979) 440.
[23] D.J. Rose Jr., J. Chromatogr. 540 (1991) 343.
[24] T.M. Joys, H. Kim, Anal. Biochem. 94 (1979) 371.
[25] Z. Zhao, A. Malik, M. Lee, Anal. Chem. 65 (1993) 2747.